Applied Mathematics, 2022, 13, 178-190
https://www.scirp.org/journal/am
ISSN Online: 2152-7393
ISSN Print: 2152-7385

Function Projective Synchronization between Two Discrete-Time Hyperchaotic Systems Using Backstepping Method

Xin Li

School of Mathematics and Statistics, Changshu Institute of Technology, Changshu, China
Email: lovelixin0412@163.com

How to cite this paper: Li, X. (2022) Function Projective Synchronization between Two Discrete-Time Hyperchaotic Systems Using Backstepping Method. *Applied Mathematics*, **13**, 178-190.
https://doi.org/10.4236/am.2022.132014

Received: January 11, 2022
Accepted: February 20, 2022
Published: February 23, 2022

Abstract

We realize the function projective synchronization (FPS) between two discrete-time hyperchaotic systems, that is, the drive state vectors and the response state vectors can evolve in a proportional scaling function matrix. In this paper, a systematic scheme is explored to investigate the function projective synchronization of two identical discrete-time hyperchaotic systems using the backstepping method. Additionally, FPS of two different hyperchaotic systems is also realized. Numeric simulations are given to verify the effectiveness of our scheme.

Keywords

Function Projective Synchronization, Discrete-Time Hyperchaotic System, Backstepping Method

1. Introduction

Many researchers have been dealing with synchronizing chaotic dynamical systems extensively [1] [2] [3]. Due to potential applications, many types of chaos synchronization in dynamical systems such as complete, phase, lag, cluster, and anticipated synchronization, etc [4] [5] [6] [7] [8] are widely investigated. Especially, amongst all kinds of chaos synchronization, the projective synchronization reported by Mainieri and Rehacek is one of the most noticeable ones that the drive and response vectors evolve proportionally in a scale matirx [9]. The projective synchronization is usually reported only in partial-linearity systems early. Subsequently, the projective synchronization is extended to non-partially-linear systems [10]-[15].

Because of much more complicated structure and higher unpredictability, hyperchaotic systems have been broadly applied in secure communications [16], lasers [17], optimal control [18], and so on. Many researchers investigate chaos (hyperchaotic) synchronization in continuous-time systems using different methods. However, many mathematical models are defined with discrete-time dynamical systems [19] [20] [21] [22]. Therefore, more and more attention is paid to the synchronization and control in discrete-time chaotic systems, especially in discrete-time hyperchaotic systems.

Backstepping design method [23] [24] plays a very important role in constructing the associated Lyapunov functions and feedback controllers. In this paper, we investigate the function projective synchronization (FPS) by exploring a systematic and automatic algorithm [22], by which the discrete-time drive system and response system, whether is with strict-feedback form or not, can be projectively synchronized via suitable controllers. By means of symbolic-numeric computation, the proposed scheme is used to realize FPS of 3D discrete-time hyperchaotic systems between two identical Rösler systems [25], and two different systems of Rösler system and the Henon system [26], respectively. Moreover, numerical simulations are given to verify the availability of the proposed scheme.

The rest of this paper is organized as follows. In Section 2, the definition of FPS in discrete-time hyperchaotic systems and the Lyapunov stability theory are introduced. In Section 3, we first illustrate the general theory of FPS in two identical Rössler hyperchaotic discrete-time systems, and then give the numerical simulation of the associated results. We also discuss the FPS of the two different discrete-time hyperchaotic systems (the Henon hyperchaotic system and the Rössler hyperchaotic system) in Section 4. Finally, some conclusions and discussions are given in Section 5.

2. Function Projective Synchronization between Two Discrete-Time Chaotic Systems

In this section, we give the conception of FPS in discrete-time hyperchaotic dynamical systems as we defined earlier [15].

Consider the two hyperchaotic systems in discrete-time style, which are described as follows: the drive system (a) $X(k+1)=F(X(k))$, and the response system with controllers (b) $Y(k+1)=G(Y(k))+u(X(k),Y(k))$. Where $X(k)=(x_1(k),x_2(k),x_3(k))$, $Y(k)=(y_1(k),y_2(k),y_3(k))$, $k\in Z/Z^-$, $u(X(k),Y(k))\in R^3$. Additionally, (c) the error system

$$E(k)=(E_1(k),E_2(k),E_3(k))$$
$$=(x_1(k)-f_1(X(k))y_1(k),x_2(k)-f_2(X(k))y_2(k),x_3(k)-f_3(X(k))y_3(k)).$$

If there exist suitable controllers $u(x(k),y(k))=(u_1(X(k),Y(k)),u_2(X(k),Y(k)),u_3(X(k),Y(k)))$, satisfying $\lim_{k\to\infty}(E(k))=0$, one can say that there exists **function projective synchronization (FPS)** in the above drive (a) and response systems (b).

Furthermore, consider the error discrete-time (c) generated by the drive system (a) and the response system (b). Let $L(E_1(k),\cdots,E_4(k))\big|_{E_i(k)\equiv 0(i=1,2,3)}=0$, when $\Delta L(k)=L(k+1)-L(k)\le 0$, with the equality holding if and only if

$E_i(k) \equiv 0 (i = 1,2,3)$, we can say that systems (a) and (b) are function projective synchronized, according to the Lyapunov stability theory.

Here we would like to point out that the controller u desponds on the synchronization method chosen. In fact, when $E_i(k) \equiv 0 (i = 1,2,3)$, $u = (f^{-1}) F - G$, where $f = diag(f_1(x(k)), f_2(x(k)), f_3(x(k)))$. That is to say, $u = (f^{-1}) F - G$ is the situation when all the error functions equal to zero and the corresponding controller is trivial situation. For $E_i(k) = 0$, we need only to solve the equations

$$\begin{aligned}&(E_1(k), E_2(k), E_3(k))\\&= (x_1(k) - f_1(X(k)) y_1(k), x_2(k) - f_2(X(k)) y_2(k), x_3(k) - f_3(X(k)) y_3(k))\\&= (0,0,0)\end{aligned}$$

to obtain the trivial controller "u". Therefore, here we just regard the general condition $\lim_{k\to\infty}(E(k)) = 0$.

In this paper, we would like to propose a systematic and constructive scheme to search the controllers between 3D hyperchaotic discrete-time systems [25] [26] with strict-feed form are function projective synchronized.

3. FPS between Two Identical Three-Dimensional Discrete-Time Hyperchaotic Systems

In this section, we consider the FPS of two identical Rössler hyperchaotic systems [25]. The discrete-time drive and response systems are described as following:

$$\begin{aligned}x_1(k+1) &= a_3\delta x_2(k) + (a_4\delta + 1) x_1(k),\\x_2(k+1) &= a_2\delta x_3(k) + a_1\delta x_1(k) + x_2(k),\\x_3(k+1) &= a_5\delta + a_6\delta x_2(k) x_3(k) + (a_7\delta + 1) x_3(k),\end{aligned} \tag{1}$$

and

$$\begin{aligned}y_1(k+1) &= a_3\delta y_2(k) + (a_4\delta + 1) y_1(k) + u_1,\\y_2(k+1) &= a_2\delta y_3(k) + a_1\delta y_1(k) + y_2(k) + u_2,\\y_3(k+1) &= a_5\delta + a_6\delta y_2(k) y_3(k) + (a_7\delta + 1) y_3(k) + u_3.\end{aligned} \tag{2}$$

As we all know, the dynamic system will have different dynamic behavior when choosing different parameter values. When $a_1 = -1.9$, $a_2 = 0.2$, $a_3 = 0.5$, $a_4 = -2.3$, $a_5 = 2$, $a_6 = -0.6$, $a_7 = -1.9$ and $\delta = 1$, hyperchaos occurs in both the systems (1) and (2) without the controllers. In this section, we choose the values of the parameters in the systems (1) and (2) as the above values. The synchronization process for the above discrete-time dynamical systems, with the powerful Lyapunov stability theory and backstepping design method is introduced in detail as follows. We select $(f_1(x), f_2(x), f_3(x)) = (2, 1 + \tanh(x_1(k)), -2)$. So the error states should be $E_1(k) = x_1(k) - 2y_1(k)$, $E_2(k) = x_2(k) - (1 + \tanh(x_1(k))) y_2(k)$, $E_3(k) = x_3(k) - x_2(k) y_3(k)$. Substituting (1) and (2) into the above error states, we can obtain the discrete-time error dynamical system

$$
\begin{aligned}
E_1(k+1) &= a_3\delta x_2(k)+(a_4\delta+1)x_1(k)-2a_3\delta y_2(k) \\
&\quad -2(a_4\delta+1)y_1(k)-2u_1(x,y), \\
E_2(k+1) &= -\left(1+\tanh\left(a_3\delta x_2(k)+(a_4\delta+1)x_1(k)\right)\right)\left(a_2\delta y_3(k)+a_1\delta y_1(k)\right. \\
&\quad \left.+y_2(k)+u_2(x,y)\right)+a_2\delta x_3(k)+a_1\delta x_1(k)+x_2(k), \\
E_3(k+1) &= a_6\delta x_2(k)x_3(k)+(a_7\delta+1)x_3(k)+2a_6\delta y_2(k)y_3(k) \\
&\quad +2(a_7\delta+1)y_3(k)+3a_5\delta+2u_3(x,y).
\end{aligned}
\tag{3}
$$

3.1. General Theory

According to the improved backstepping method [27] and Lyapunov stability theory, a systematic and constructive algorithm to derive the controllers $u(x,y)$ will be given step by step, in order to realize the FPS between the systems (1) and (2).

Theorem 1: (Lyapunov's Stability Theory) Let $x=0$ be an equilibrium for $\dot{x}=f(x)$ and $D\subset R^n$ be invariant, and let $V:D\to R$ be a continuously differentiable function such that: when $x\in D\setminus\{0\}$, $V(0)=0$ and $V(x)>0$; when $x\in D$, $\dot{V}(0)\le 0$. Then $x=0$ is stable. Moreover, when $x\in D\setminus\{0\}$, $\dot{V}(x)<0$, then $x=0$ is asymptotically stable.

Here we extent the above theory to the discret-time hyperchaotic systems.

Step 1. Let the first partial Lyapunov function be $L_1(k)=|E_1(k)|$ and the second error variable be

$$E_2(k)=E_1(k+1)-c_{11}E_1(k). \tag{4}$$

Then we can obtain the derivative of $L_1(k)$

$$\Delta L_1(k)=|E_1(k+1)|-|E_1(k)|\le(|c_{11}|-1)|E_1(k)|+|E_2(k)|. \tag{5}$$

Step 2. The third error variable is described as

$$E_3(k)=E_2(k+1)-c_{21}E_1(k)-c_{22}E_2(k). \tag{6}$$

And the derivative of $L_2(k)$ is defined as follows

$$\Delta L_2(k)=|E_2(k+1)|-|E_2(k)|\le c_{21}E_1(k)+(|c_{22}|-1)|E_2(k)|+|E_3(k)|. \tag{7}$$

Step 3. Let

$$E_3(k+1)-c_{31}E_1(k)-c_{32}E_2(k)-c_{33}E_3(k)=0. \tag{8}$$

With the help of symbolic computation and the associated stability theory, it is not difficult to get the controllers from the above Equations (4) to (8).

$$
\begin{aligned}
u_1(x,y) &= \frac{1}{2}\left[y_2(k)-x_2(k)+y_2(k)\tanh(x_1(k))-c_{11}x_1(k)+a_3\delta x_2(k)\right. \\
&\quad \left.+a_4\delta x_1(k)+x_1(k)\right]+c_{11}y_1(k)-a_3\delta y_2(k)-a_4\delta y_1(k)-y_1(k), \\
u_2(x,y) &= \left(a_2\delta x_3(k)+a_1\delta x_1(k)+x_2(k)-a_2\delta y_3(k)-y_2(k)+x_1(k)a_1\delta y_1(k)\right. \\
&\quad -a_1\delta y_1(k)-\tanh\left(a_3\delta x_2(k)+a_4\delta x_1(k)+a_2\delta x_1(k)\right)y_3(k) \\
&\quad -\tanh\left(a_3\delta x_2(k)+x_1(k)a_4\delta+c_{22}y_2(k)-\tanh\left(a_3\delta x_2(k)+x_1(k)a_4\delta\right.\right. \\
&\quad \left.\left.+x_1(k)\right)y_2(k)-c_{21}x_1(k)+2c_{21}y_1(k)-c_{22}x_2(k)+c_{22}y_2(k)\tanh(x_1(k))\right) \\
&\quad \left.-x_3(k)-2y_3(k)\right)\Big/\left(1+\tanh\left(a_3\delta x_2(k)+x_1(k)a_4\delta+x_1(k)\right)\right),
\end{aligned}
$$

$$
\begin{aligned}
u_3(x,y) = & \frac{1}{2}\left[c_{31}x_1(k)+c_{32}x_2(k)-c_{32}y_2(k)-c_{32}y_2(k)\tanh\left(x_1(k)\right)+c_{33}x_3(k)\right. \\
& \left.-a_6\delta x_2(k)x_3(k)-a_7\delta x_3(k)-x_3(k)\right]-c_{31}y_1(k)+c_{33}y_3(k) \\
& -a_6\delta y_2(k)y_3(k)-a_7\delta y_3(k)-y_3(k)-3a_5\delta
\end{aligned} \tag{9}
$$

Then suppose the Lyapunov function be $L(k)=\left|E_1(k)\right|+d_1\left|E_2(k)\right|+d_2\left|E_3(k)\right|$, $d_2>d_1>1$. We get the derivative of the Lyapunov function $L(k)$ from (4) and (7) as following

$$
\begin{aligned}
\Delta L(k) &= L(k+1)-L(k) \\
& \le \left(d_2\left|c_{31}\right|+d_1\left|c_{21}\right|+\left|c_{11}\right|-1\right)\left|E_1(k)\right|+\left(d_2\left|c_{32}\right|+d_1\left(\left|c_{22}\right|-1\right)+1\right)\left|E_2(k)\right| \\
& \quad +\left(d_2\left|c_{33}\right|+d_1-d_2\right)\left|E_2(k)\right|.
\end{aligned} \tag{10}
$$

We choose the appropriate values for these constants $c_{11},c_{21},c_{22},c_{31},c_{32},c_{33}$ to satisfy

$$
\begin{aligned}
& d_1\left|c_{21}\right|+d_2\left|c_{31}\right|+\left|c_{11}\right|<1, \\
& d_1\left|c_{22}\right|+d_2\left|c_{32}\right|<d_1-1, \\
& \left|c_{33}\right|<\frac{d_2-d_1}{d_2}.
\end{aligned} \tag{11}
$$

Therefore, $\Delta L(k)$ is negative definite which means that the close-loop discrete-time system

$$
\begin{pmatrix} E_1(k+1) \\ E_2(k+1) \\ E_3(k+1) \end{pmatrix} = \begin{pmatrix} c_{11} & 0 & 0 \\ c_{21} & c_{22} & 0 \\ c_{31} & c_{32} & c_{33} \end{pmatrix} \begin{pmatrix} E_1(k) \\ E_2(k) \\ E_3(k) \end{pmatrix}
$$

is globally asymptotically stable and $\lim_{k\to+\infty} E_i(k)=0$. So discrete-time hyperchaotic system (1) and (2) are function projective synchronized.

3.2. Numerical Simulation Results

In this subsection, some numerical simulations are used to verify the effectiveness of the obtained controllers $u(x,y)$. Here we choose $c_{11}=0.3$, $c_{21}=0.02$, $c_{22}=0.4$, $c_{31}=0.05$, $c_{32}=0.1$, $c_{33}=-0.2$, $d_1=4$, $d_2=6$, such that the corresponding $\Delta L(k)\le 0$, according to the condition equations in (11). Otherwise, we choose the parameters in the systems (1) and (2) as $a_1=-1.9$, $a_2=0.2$, $a_3=0.5$, $a_4=-2.3$, $a_5=2$, $a_6=-0.6$, $a_7=-1.9$ and $\delta=1$, and the corresponding initial values [$x_1(0)=0.1$, $x_2(0)=0.2$, $x_3(0)=0.3$] and [$y_1(0)=-0.1$, $y_2(0)=-0.2$, $y_3(0)=-0.3$], respectively. The pictures of the error states are displayed in **Figures 1(a)-(c)**. Obviously, E_1, E_2 and E_3 converge to zero finally after the controllers are activated. This is to say, all the state variables tend to be synchronized in the function proportion $\left(2,1+\tanh\left(x_1(k)\right),-2\right)$. And the attractors of the two systems with controllers are shown in **Figure 2**. Then in **Figures 3(a)-(c)**, we respectively put the trajectories of the response system with the controllers and the trajectories of the drive system in the same plane, and it is not difficult to find that ratio of the amplitudes of the two systems is a function scaling factor.

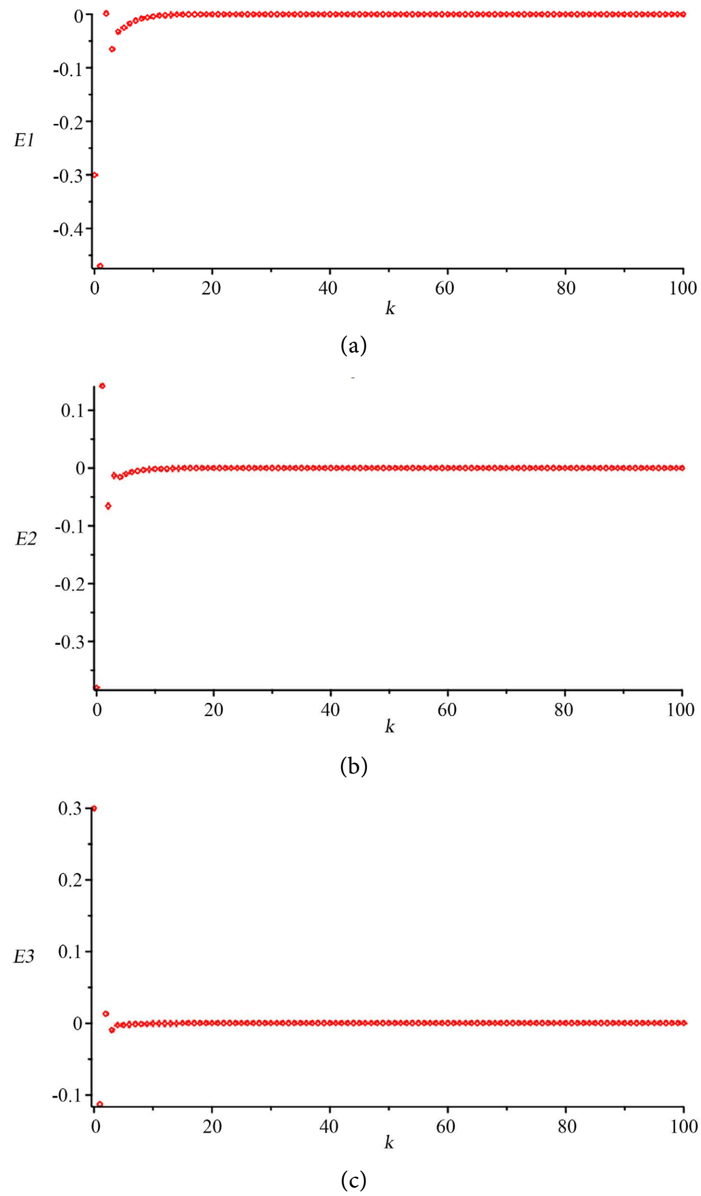

Figure 1. The orbits of the error states. (a) The orbit of E_1; (b) The orbit of E_2; (c) the orbit of E_3.

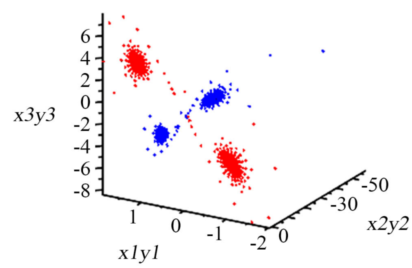

Figure 2. The two systems after being synchronized with $(f_1(x), f_2(x), f_3(x)) = (2, 1+\tanh(x_1(k)), -2)$: the blue one denotes the trajectory of the response system with the controllers, and the red one denotes the trajectory of the drive system.

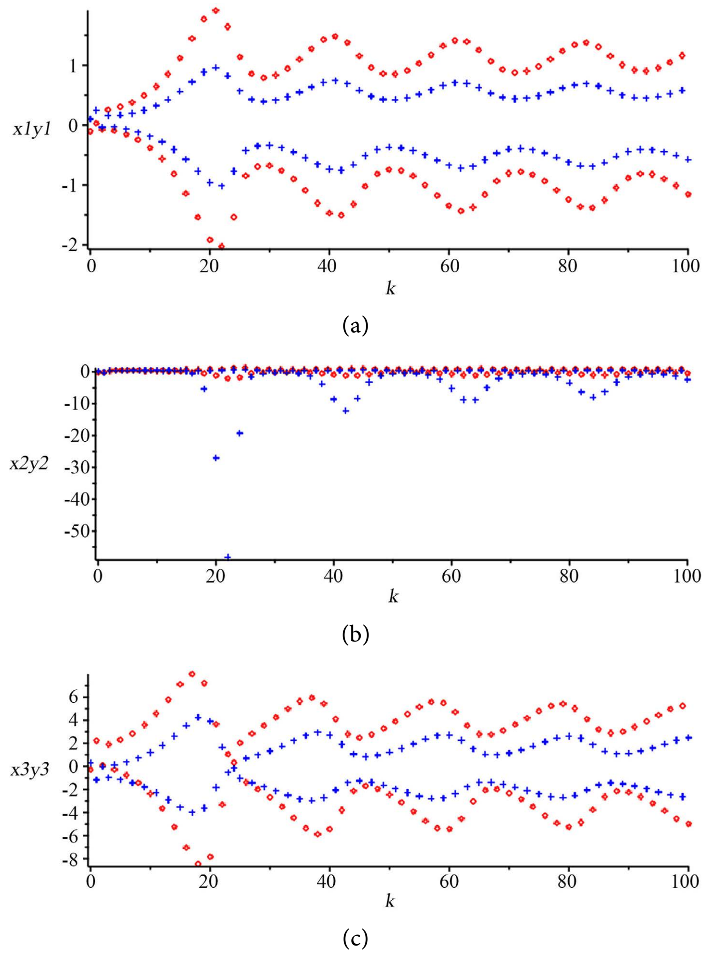

Figure 3. Characteristics of $x_i(k)$ and $y_i(k)(i=1,2,3)$ versus $t(k)$: the red circle orbits denote for $x_i(k)$ of the drive system and the blue cross orbits denote for $y_i(k)$ of the response system.

4. FPS between Two Different Three-Dimensional Discrete-Time Hyperchaotic Systems

We now consider FPS between the Henon-like map [26] and the above hyperchaotic system (1). Here we choose Henon-like map as drive system and hyperchaotic Rössler system as response system to realize FPS of two different chaotic dynamic systems with the backstepping method. The drive system and the response system with controllers are rewritten as follows: the drive system

$$\begin{aligned} x_1(k+1) &= 1 + x_3(k) - \alpha x_2^2(k), \\ x_2(k+1) &= 1 + \beta x_2(k) - \alpha x_1^2(k), \\ x_3(k+1) &= \beta x_1(k). \end{aligned} \tag{12}$$

and the response system

$$\begin{aligned} y_1(k+1) &= a_3\delta y_2(k) + (a_4\delta + 1)y_1(k) + u_1, \\ y_2(k+1) &= a_2\delta y_3(k) + a_1\delta y_1(k) + y_2(k) + u_2, \\ y_3(k+1) &= a_5\delta + a_6\delta y_2(k)y_3(k) + (a_7\delta + 1)y_3(k) + u_3. \end{aligned} \tag{13}$$

The projections of the hyperchaotic attrator of systems (12) and (1) are displayed in Figure 4(a) and Figure 4(b), respectively.

Then we also use the backstepping design method to realize the FPS of the two different discrete-time hyperchaotic systems (12) and (1). Here we choose $\left(f_1(x), f_2(x), f_3(x)\right) = \left(-1, -\frac{1}{1+x_1^2(k)}, -1\right)$, that is to say

$$\begin{aligned} E_1(k) &= x_1(k) + y_1(k), \\ E_2(k) &= x_2(k) + \frac{1}{1+x_1^2(k)} y_2(k), \\ E_3(k) &= x_3(k) + y_3(k). \end{aligned} \tag{14}$$

According to (12) and (13), we can obtain the error dynamical system

$$\begin{aligned} E_1(k+1) &= -\alpha x_2^2(k) + x_3(k) + 1 + a_3\delta y_2(k) + (a_4\delta+1) y_1(k) + u_1, \\ E_2(k+1) &= -\alpha x_1^2(k) + \beta x_2(k) + 1 + \frac{a_1\delta y_1(k) + a_2\delta y_3(k) + u_2 + y_2(k)}{\left(-\alpha x_2(k)^2 + x_3^2(k) + 1\right)^2 + 1}, \\ E_3(k+1) &= \beta x_1(k) + a_5\delta + a_6\delta y_2(k) y_3(k) + (a_7\delta+1) y_3(k) + u_3. \end{aligned} \tag{15}$$

Based on the steps of backstepping methods [27] with the above Equations (4) to (8), we have the controllers

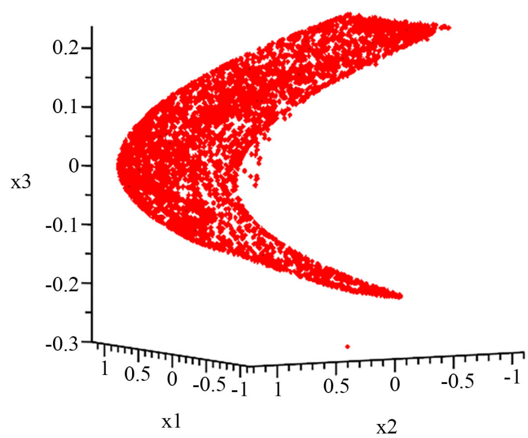

(a)

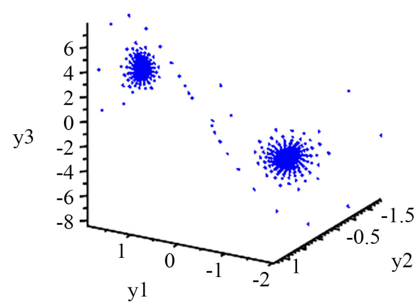

(b)

Figure 4. Phase portraits of the hyperchaotic systems: (a) The orbit of the drive system (12); (b) The orbit of the response system (1).

$$
\begin{aligned}
u_1 = & -\left(a_3\delta x_1^2(k)y_2(k)+a_4\delta x_1^2(k)y_1(k)-\alpha x_1^2(k)x_2^2(k)\right)+y_1(k)-y_2(k) \\
& +a_4\delta y_1(k)-\alpha x_2^2(k)-x_1^2(k)x_2(k)+x_1^2(k)x_3(k)+x_1^2(k)y_1(k)+x_1^2(k) \\
& +a_3\delta y_2(k)-x_2(k)+x_3(k)-c_{11}x_1(k)-c_{11}y_1(k)-c_{11}x_1^2(k)y_1(k+1) \\
& -c_{11}x_1^3(k)\big)\big/\left(x_1^2(k)+1\right), \\
u_2 = & -\big(2-2\alpha x_1^2(k)x_2^2(k)+a_2\delta y_3(k)-c_{21}x_1^3(k)x_3^2(k)-2c_{21}x_1^3(k)x_3(k) \\
& -2c_{21}x_1^2(k)y_1(k)-c_{21}x_1(k)x_3^2(k)-c_{21}x_3^2(k)y_1(k)-2c_{21}x_3(k)y_1(k) \\
& -2c_{22}x_3(k)y_2(k)-\alpha^2x_2^4(k)x_3(k)+2\alpha x_2^2(k)x_3^2(k)-x_1^2(k)x_3^2(k)y_3(k) \\
& +2\alpha x_2^2(k)y_3(k)-2x_1^2(k)x_3(k)y_3(k)-\alpha^3x_1^4(k)x_2^4(k)-\alpha^3x_1^2(k)x_2^4(k) \\
& -\alpha x_1^4(k)x_3^2(k)+2\alpha^2x_1^2(k)x_2^2(k)-2\alpha x_1^4(k)x_3(k)-2\alpha x_1^2(k)x_3(k) \\
& +2\beta x_1^2(k)x_2(k)+\beta x_2(k)x_3^2(k)+2\beta x_2(k)x_3(k)+2\alpha x_1^2(k)x_2^2(k)x_3^2(k) \\
& +2\beta x_2(k)-2\alpha x_1^2(k)-\alpha^2c_{21}x_1^2(k)x_2^4(k)y_1(k)+2\alpha c_{21}x_1^3(k)x_2^2(k)x_3(k) \\
& +2\alpha c_{21}x_1(k)x_2^2(k)x_3(k)+2\alpha c_{21}x_2^2(k)x_3(k)y_1(k) \\
& +2\alpha c_{22}x_1^2(k)x_2^3(k)x_3(k)+2\alpha x_1^2(k)x_2^2(k)x_3(k)y_3(k) \\
& -2\alpha\beta x_1^2(k)x_2^3(k)x_3(k)-\alpha^2c_{21}x_1(k)x_2^4(k)-\alpha^2c_{21}x_2^4(k)y_1(k) \\
& +2\alpha c_{21}x_1^3(k)x_2^2(k)-c_{21}x_1^2(k)x_3^2(k)y_1(k)-2c_{21}x_1^3(k) \\
& -2c_{21}x_1^2(k)x_3(k)y_1(k)-\alpha^2c_{22}x_1^2(k)x_2^5(k)-\alpha^2c_{22}x_2^4(k)y_2(k)-2\alpha x_1^4(k) \\
& -c_{22}x_1^2(k)x_2(k)x_3^2(k)+2\alpha c_{22}x_2^2(k)y_2(k)-2c_{22}x_1^2(k)x_2(k)x_3(k) \\
& -2c_{22}y_2(k)-\alpha^2x_1^2(k)x_2^4(k)y_3(k)+2\alpha x_1^2(k)x_2^2(k)y_3(k) \\
& +2\alpha x_2^2(k)x_3(k)y_3(k)-2c_{22}x_2(k)+\alpha^2\beta x_1^2(k)x_2^5(k)-2\alpha\beta x_1^2(k)x_2^3(k) \\
& -2\alpha\beta x_2^3(k)x_3(k)+\beta x_1^2(k)x_2(k)x_3^2(k)+a_1\delta x_1^2(k)y_1(k) \\
& +a_2\delta x_1^2(k)y_3(k)-x_3^3(k)-x_3^2(k)-2x_1^2(k)y_3(k)-2c_{21}x_1(k)-2c_{21}y_1(k) \\
& -x_1^2(k)x_3^3(k)-x_1^2(k)x_3^2(k)+2\alpha^2x_1^2(k)x_2^2(k)x_3(k)-x_3^2(k)y_3(k) \\
& -2x_3(k)y_3(k)+\alpha^2x_2^4(k)+x_1^2(k)y_2(k)+a_1\delta y_1(k)+y_2(k) \\
& -2c_{22}x_2(k)x_3(k)-2c_{21}x_1(k)x_3(k)-\alpha^2x_2^4(k)y_3(k)+2\alpha^2x_1^4(k)x_2^2(k) \\
& -2\alpha x_2^2(k)-2\alpha\beta x_2^3(k)-\alpha x_1^2(k)x_3^2(k)+\alpha^2\beta x_2^5(k)+\alpha^2x_1^2(k)x_2^4(k) \\
& +2x_1^2(k)+2\alpha c_{21}x_1^2(k)x_2^2(k)y_1(k)+2\alpha c_{22}x_2^2(k)x_3(k)y_2(k)-2y_3(k) \\
& -\alpha^2c_{21}x_1^3(k)x_2^4(k)+2\alpha c_{21}x_1(k)x_2^2(k)+2\alpha c_{21}x_2^2(k)y_1(k) \\
& -\alpha^2x_1^2(k)x_2^4(k)x_3(k)+2\alpha^2x_1^4(k)x_2^2(k)x_3(k)+2\beta x_1^2(k)x_2(k)x_3(k) \\
& +2\alpha c_{21}x_1^2(k)x_2^2(k)x_3(k)y_1(k)\big)\big/\left(x_1^2(k)+1\right), \\
u_3 = & -\big(a_6\delta x_1^2(k)y_2(k)y_3(k)+a_7\delta x_1^2(k)y_3(k)+a_5\delta x_1^2(k)+\beta x_1^3(k) \\
& -c_{31}x_1^3(k)+a_6\delta y_2(k)y_3(k)-c_{31}x_1^2(k)y_1(k)-c_{32}x_1^2(k)x_2(k) \\
& -c_{33}x_1^2(k)x_3(k)+a_7\delta y_3(k)-c_{33}x_1^2(k)y_3(k)+x_1^2(k)y_3(k)+a_5\delta \\
& +\beta x_1(k)-c_{31}x_1(k)-c_{31}y_1(k)-c_{32}x_2(k)-c_{32}y_2(k)-c_{33}x_3(k) \\
& -c_{33}y_3(k)+y_3(k)+2\alpha c_{22}x_1^2(k)x_2^3(k)+2\alpha c_{22}x_2^3(k)x_3(k)\big)
\end{aligned}
\tag{16}
$$

Here numerical simulations are also used to verify the effectiveness of the obtained controllers $u(x,y)$ above. Without losing generality, we take the same parameter values of $c_{11}, c_{21}, c_{22}, c_{31}, c_{32}, c_{33}, d_1, d_2$ in section 3, and take the initial values as [$x_1(0)=0.1$, $x_2(0)=0.2$, $x_3(0)=0.3$] and [$y_1(0)=-0.5$, $y_2(0)=0.2$, $y_3(0)=0.1$], respectively. The figures of the error states are shown in **Figures 5(a)-(c)**. That is easy to see, all the three orbits of $E_i\ (i=1,2,3)$ converge to zero finally after the controllers u_1, u_2, u_3 are activated. So all the state variables tend to be synchronized in proportion $\left(-1, -\frac{1}{1+x_1^2(k)}, -1\right)$. The attractors of the two systems with controllers tending to a function scaling factor, are displayed in **Figure 6**.

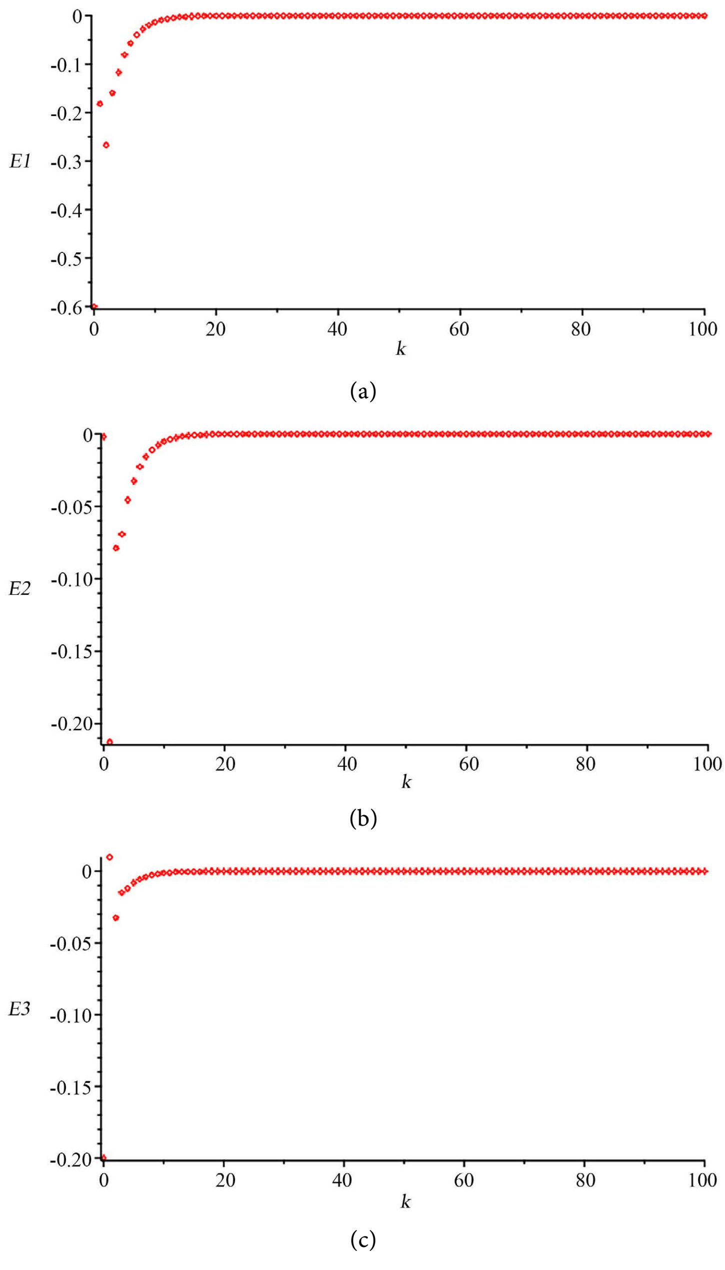

Figure 5. The trajectories of the error states. (a) The orbit of E_1; (b) The orbit of E_2; (c) The orbit of E_3.

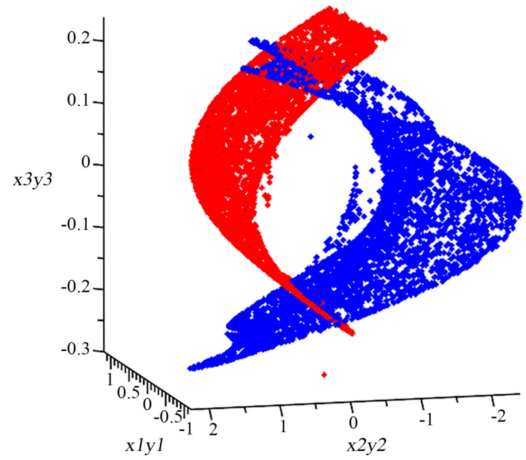

Figure 6. The two systems after being synchronized with $\left(f_1(x), f_2(x), f_3(x)\right) = \left(-1, -\frac{1}{1+x_1^2(k)}, -1\right)$: the red one is the drive system with the controllers, and the blue one is the response system.

5. Conclusion

In conclusion, the conception of the function projective synchronization between discrete-time hyperchaotic dynamical systems is presented. According to backstepping design method with controllers, a systematic, automatic and constructive scheme is explored in order to investigate FPS between the discrete-time drive systems and response systems, whether is in strict-feedback forms or not. Additionally, the proposed scheme is used to realize the function of projective synchronization between the identical discrete-time hyperchaotic systems from Rössler system and two different hyperchaotic systems which are the hyperchaotic Rössler system and the Henon map, respectively. With the aid of symbolic computation *Maple*, the numerical simulations are shown to perform the process of the synchronization and the effectiveness of the above-designed controller successfully.

Acknowledgements

This work is supported by Natural Science Foundation for the Youth of Jiangsu Province (No. BK20181030), National Natural Science Foundation for the Youth of China (No. 12101084), and Jiangsu Overseas Visiting Scholar Program for University Prominent Young and Middle-aged Teachers and Presidents.

Conflicts of Interest

The author declares no conflicts of interest regarding the publication of this paper.

References

[1] Ott, E., Grebogi, C. and Yorke, J.A. (1990) Controlling Chaos. *Physical Review Letters*, **64**, 1196-1199. https://doi.org/10.1103/PhysRevLett.64.1196

[2] Wang, H., Ye, J.M., Miao, Z.H. and Jonckheere, E.A. (2018) Robust Finite-Time Chaos Synchronization of Time-Delay Chaotic Systems and Its Application in Secure Communication. *Transactions of the Institute of Measurement and Control*, **40**, 1177-1187. https://doi.org/10.1177/0142331216678311

[3] Hamel, S. and Boulkroune, A. (2016) A Generalized Function Projective Synchronization Scheme for Uncertain Chaotic Systems Subject to Input Nonlinearities. *International Journal of General Systems*, **45**, 689-710. https://doi.org/10.1080/03081079.2015.1118094

[4] Boccaletti, S., Kurth, J., Osipov, G., Valladares, D.L. and Zhou, C.S. (2002) The Synchronization of Chaotic Systems. *Physics Reports*, **366**, 1-101. https://doi.org/10.1016/S0370-1573(02)00137-0

[5] Al-Azzawi, S.F. and Aziz, M.M. (2018) Chaos Synchronization of Nonlinear Dynamical Systems via a Novel Analytical Approach. *Alexandria Engineering Journal*, **57**, 3493-3500. https://doi.org/10.1016/j.aej.2017.11.017

[6] Chen, G.R. and Dong, X.N. (1998) From Chaos to Order: Methodologies, Perspectives and Applications. World Scientific, Singapore. https://doi.org/10.1142/3033

[7] Yan, Z.Y. (2005) Q-S (Lag or Anticipated) Synchronization Backstepping Scheme in a Class of Discrete-Time Chaotic (Hyperchaotic) Systems: A Symbolic-Numeric Computation Approach. *Chaos*, **15**, Article ID: 023902. https://doi.org/10.1063/1.1876612

[8] Yang, S., Hu, C., Yu, J. and Jiang, H.J. (2021) Exponential Synchronization of Fractional-Order Reaction-Diffusion Coupled Neural Networks with Hybrid Delay-Dependent Impulses. *Journal of the Franklin Institute*, **358**, 3167-3192.

[9] Mainieri, R. and Rehacek, J. (1999) Projective Synchronization in Three-Dimensional Chaotic Systems. *Physical Review Letters*, **82**, 3042-3045. https://doi.org/10.1103/PhysRevLett.82.3042

[10] Li, G.H. (2007) Generalized Projective Synchronization between Lorenz System and Chen's System. *Chaos*, *Solitons & Fractals*, **32**, 1454-1458. https://doi.org/10.1016/j.chaos.2005.11.073

[11] Chen, Y. and Li, X. (2007) Function Projective Synchronization between Two Different Chaotic Systems. *Zeitschrift für Naturforschung A*, **62**, 29-33. https://doi.org/10.1515/zna-2007-1-205

[12] Chen, Y. and Li, X. (2007) Function Projective Synchronization between Two Identical Chaotic Systems. *International Journal of Modern Physics C*, **18**, 883-888. https://doi.org/10.1142/S0129183107010607

[13] Li, X. and Chen, Y. (2007) Generalized Projective Synchronization between Rössler System and New Unified Chaotic System. *Communications in Theoretical Physics*, **48**, 132-136. https://doi.org/10.1088/0253-6102/48/1/027

[14] Qiu, X.L., Bin, H.H. and Chu, L.C. (2017) Modified Function Projective Synchronization of Complex Networks with Multiple Proportional Delays. *Applied Mathematics*, **8**, 537-549. https://doi.org/10.4236/am.2017.84043

[15] Li, X. and Chen, Y. (2009) Stabilizing of Two-Dimensional Discrete Lorenz Chaotic System and Three-Dimensional Discrete Rössler Hyperchaotic System. *Chinese Physics Letters*, **26**, Article ID: 090503. https://doi.org/10.1088/0256-307X/26/9/090503

[16] Li, C.D., Liao, X.F. and Wong, K.W. (2005) Lag Synchronization of Hyperchaos with Application to Secure Communications. *Chaos*, *Solitons & Fractals*, **23**, 183-193. https://doi.org/10.1016/j.chaos.2004.04.025

[17] Vicente, R., Dauden, J., Colet, P. and Toral, R. (2005) Analysis and Characterization of the Hyperchaos Generated by a Semiconductor Laser Subject to a Delayed Feedback Loop. *IEEE Journal of Quantum Electronics*, **41**, 541-548. https://doi.org/10.1109/JQE.2005.843606

[18] Baleanu, D., Jajarmi, A., Sajjadi, S.S. and Mozyrska, D. (2019) A New Fractional Model and Optimal Control of a Tumor-Immune Surveillance with Non-Singular Derivative Operator. *Chaos*: *An Interdisciplinary Journal of Nonlinear Science*, **29**, Article ID: 083127. https://doi.org/10.1063/1.5096159

[19] Itoh, M. and Chua, L.O. (2003) Equivalent CNN Cell Models and Patterns. *International Journal of Bifurcation and Chaos*, **13**, 1055-1161. https://doi.org/10.1142/S0218127403007151

[20] Wang, X. Y. (2003) Chaos in Complex Nonlinear Systems. Publishing House of Electronics Industry, Beijing.

[21] Yan, Z.Y. (2006) Q-S (Complete or Anticipated) Synchronization Backstepping Scheme in a Class of Discrete-Time Chaotic (Hyperchaotic) Systems: A Symbolic-Numeric Computation Approach. *Chaos*, **16**, Article ID: 013119. https://doi.org/10.1063/1.1930727

[22] Li, X., Chen, Y. and Li, Z.B. (2008) Function Projective Synchronization of Discrete-Time Chaotic Systems. *Zeitschrift für Naturforschung A*, **63**, 7-14. https://doi.org/10.1515/zna-2008-1-202

[23] Krstic, M., Kaneuakopoulos, I. and Kokotovic, P.V. (1995) Nonlinear Adaptive Control Design. Wiley, New York.

[24] He, P., Ma, S.H. and Fan, T. (2012) Finite-Time Mixed Outer Synchronization of Complex Networks with Coupling Time-Varying Delay. *Chaos*, **22**, Article ID: 043151. https://doi.org/10.1063/1.4773005

[25] Rössler, O.E. (1979) An Equation for Hyperchaos. *Physics Letters A*, **71**, 155-157. https://doi.org/10.1016/0375-9601(79)90150-6

[26] Yan, Z.Y. (2005) Q-S Synchronization in 3D Hénon-Like Map and Generalized Hénon Map via a Scalar Controller. *Physics Letters A*, **342**, 309-317. https://doi.org/10.1016/j.physleta.2005.04.049

[27] Wu, G.C., Baleanu, D., Xie, H.P. and Chen, F.L. (2016) Chaos Synchronization of Fractional Chaotic Maps Based on the Stability Condition. *Physica A*: *Statistical Mechanics and its Applications*, **460**, 374-383. https://doi.org/10.1016/j.physa.2016.05.045